5. Scanning BRILLOUIN microscopic studies of interface-induced properties in polymers

This chapter aims at demonstrating that scanning BRILLOUIN microscopy leads to a unique perspective on interface-induced properties of semi-crystalline and amorphous network-forming polymers. Manifold phenomena such as the transcrystallisation of spherulithes (SCHULTZ 1974, BARTENEV & ZELENEV 1979, STROBL 2007) within a partially crystalline polymer close to a metallic surface and the influence of polymerization-induced stresses within an epoxy adhesive glued to different metallic substrates will be studied at hypersonic frequencies. Furthermore the network formation of an adhesive polymerizing in the vicinity of a boundary selective for the reactants and several transport processes of solvents penetrating into polymeric networks will be discussed. The common point of all of these diverse long-ranged processes is that they are originally induced at the planar phase boundary between the investigated polymer and its counterpart.

5.1. Surface-induced crystallisation of a semi-crystalline polymer

The complex spherolitic structure of semi-crystalline polymers and its genesis have been debated for several decades (SCHULTZ 1974, BARTENEV & ZELENEV 1979, STROBL 2007). Some central questions concerned e.g. the degree of crystallinity, the heterogeneous distributions of the crystallites, the textures resulting from transcrystallisation starting at the sample's surfaces during manufacturing, and the flow-induced orientation of the amorphous polymeric matrix as well as of the embedded crystallites. For sure, all of these parameters can be easily influenced by the sample preparation technique. Usually, the prepared solid specimens are in thermodynamically frozen, strong non-equilibrium states, which evolve towards more stable states when annealed above the glass transition temperature. Further issues of debate concern the relationship between the morphology of polymeric materials and their properties. In this context, especially the elastic properties of solid polymers lie in the focus of basic and industrial research.

The elastic properties of partially crystalline polymers sensitively depend on the formed micro- to mesoscopic morphologies (BARTENEV & ZELENEV 1979, STROBL 2007). Particularly the mesoscopically heterogeneous structures are responsible for strong Mie scattering at optical wavelengths. Therefore, these materials are generally difficult to investigate by BRILLOUIN spectroscopy. In contrast to most semi-crystalline polymers, poly(4-methyl-1-pentene), denoted as P4MP1, is optically highly transparent. This astonishing feature results from the almost complete absence of birefringence in P4MP1 crystals (KRÜGER *et al.* 1978a). In addition, the crystalline and amorphous parts possess similar mass densities within a large temperature interval (KRÜGER *et al*. 1978a). Hence, BRILLOUIN spectroscopy is perfectly suited for the study of the acoustic or elastic properties of P4MP1 specimens. For this material, $SBM^{\theta A}$ gives an indirect access to textures of the semi-crystalline state and to a possible spatial dependence of the crystallite density.

In the late 1970s, the acoustic properties of P4MP1 films with thicknesses ranging between 18 and 200 microns were investigated by BRILLOUIN microscopy near the surface and in the middle of injection moulded or chill-rolled samples (KRÜGER *et al.* 1978a). It turned out that these samples have different hypersonic velocities across their thickness x_3, thus demonstrating their acoustic inhomogeneity. As a matter of fact, optical isotropy and homogeneity do not go along with acoustic isotropy and homogeneity for P4MP1! That this feature is not limited to P4MP1, but is more general, will be shown in section 6.2. X-ray investigations evidenced that the degree of crystallinity was about 28% for all samples and that the crystals are only slightly oriented along the roll direction. However, a possible texture across the thickness of the samples could not be resolved at these times by x-ray scattering. Obviously, SBM gives additional information: while the studied P4MP1 films were elastically isotropic in the middle, they were anisotropic in the surface-near zones. Transcrystallisation occurring in the surface-near zones provoked a slight orientation of the crystallites as evidenced by the orthorhombic symmetry of the related elastic tensor (KRÜGER *et al.* 1978a).

In 2003, an acoustic profile with a resolution of less than 10 microns was documented for a 2 mm thick injection moulded P4MP1 plate (SANCTUARY *et al.* 2003). The selected optical setup is described in detail in section 3.3. Note that for the chosen 90A scattering geometry the phonon wave vector lies within the (x_1, x_2)-plane, and hence perpendicular to the thickness of the plate. Figure 5.1 represents the related hypersonic properties across the sample thickness x_3 (SANCTUARY *et al.* 2003). Whereas the hypersonic attenuation is almost space-independent, the sound velocity v_{qL}^{90A} strongly varies along the profile. The lowest sound velocities are noticed for the surface-near zones, whereas the about 20% higher maximum values lie close to the middle of the plate. Note that only space-resolved, but not angle-resolved BRILLOUIN microscopy was applied to this sample. Figure 5.1 illustrates that interface-induced processes can easily operate over distances of several tenths of a millimetre within this semi-crystalline polymer.

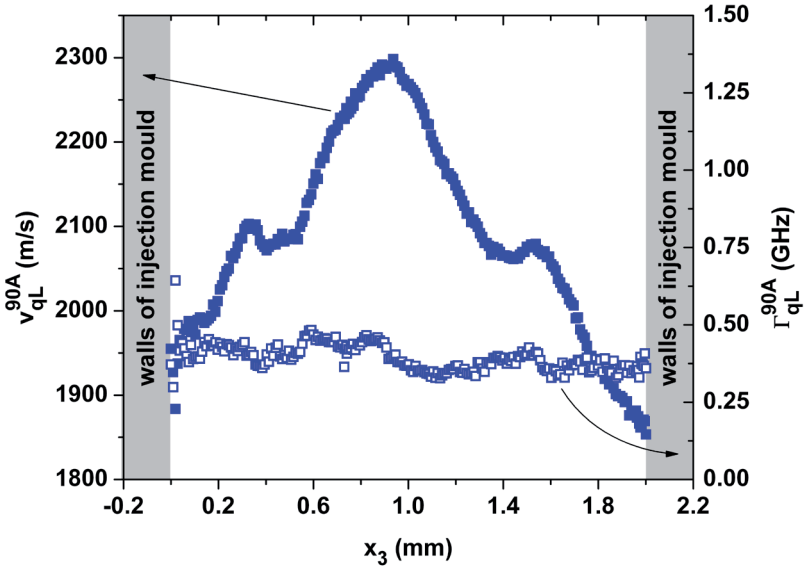

Fig. 5.1. Spatial profile of the sound velocity v_{qL}^{90A} *and hypersonic attenuation* Γ_{qL}^{90A} *across the thickness* x_3 *of an injection moulded poly(4-methyl-1-pentene) plate.*

Apparently, the observed acoustic inhomogeneity as reflected by the sound velocity profile along the sample's thickness does not affect, in the margin of error, the hypersonic attenuation. Consequently, these acoustic inhomogeneities do not result from relaxation phenomena. As the sample jumps off the mould during rapid cooling because of volume shrinkage, stresses can almost completely relax in the sample. Stresses can thus also be ruled out as the underlying reasons for the observed inhomogeneity. We conclude that the acoustic inhomogeneities are of static nature and result from morphological variations within the P4MP1 sample. An explanation looks as follows: as soon as the injected P4MP1 melt comes into contact with the walls of the much cooler mould, transcrystallization progresses from the mould-polymer interface deeper into the specimen.

Close to the mould's walls, the polymeric chains are preferentially oriented perpendicular to the walls. Hence the hightest sound velocity is measured in the direction perpendicular to the wall and the lowest sound velocitiy, parallel to the wall (as was done in this experiment). Important temperature gradients within the chilling polymer provoke further oriented growth of the crystals with a decaying crystal orientation towards the centre of the sample plate. As this sample was prepared by injection moulding, we expect away from the mould's walls flow-induced molecular orientation within the (x_1, x_2)-plane, in other words perpendicular to the chain orientation provoked at the walls by transcrystallization. These two competing processes could qualitatively explain the shape of the profile of the quasi-longitudinally polarized sound velocity: as the phonon wave vector $\vec{q}^{90A}$ lies within the (x_1, x_2)-plane, the highest sound velocity values are determined in the middle of the profile, where the molecular chains seem to be preferentially oriented rather parallel to $\vec{q}^{90A}$, but not perpendicular to it like for the transcrystallized state close to the borders. It remains unclear in how far the degree of crystallinity is possibly reduced at the sample's borders because of the fast cooling process, which of course also affects the sound velocity profile.

5.2. Mechanical properties of epoxy networks at metallic interfaces

The formation of so-called interphases (POSSART 2005, POSSART *et al*. 2006) within polymers caused by interactions at polymer-solid boundaries has raised much attention during the last years. In this section we focus on the elastic properties within interphases of adhesive epoxy-metal bonds – a crucial problematic for the aerospace and automotive industry, to name only two. From the viewpoint of mechanical properties, an adhesive bond generally needs to fulfil several criteria: first strong adhesive interaction between the adhesive and the materials selected for joining, second sufficient mechanical stability, third as slow physicochemical ageing as possible, etc (POSSART *et al.* 2006, WEHLACK *et al*. 2007).

The frequent inter-dependence of the complex physicochemical processes provoking the adhesion and the strong dependence of these processes on the chemical nature of the adhesive and the metal surfaces are jointly responsible for the currently crude understanding of adhesive bonding (POSSART 2005, POSSART *et al.* 2006, WEHLACK *et al.* 2007).

It is generally accepted in literature (e.g. POSSART 2005, POSSART *et al.* 2006, WEHLACK *et al.* 2007) that physicochemical epoxy-metal interactions lead to 'chemical interphases' in the epoxy. Compared to bulk epoxy, the latter possess modified structural and chemical properties, like chemical composition and reactivity. While typical dimensions of chemical interphases range in the nanometer length scale, the question is in how far the epoxy's morphology can be modified beyond the thickness of a possible chemical interphase by further physicochemical interactions at the phase boundary. The morphological transition zone of the epoxy between bulk epoxy and the metal surface is denoted as the 'morphological interphase'. In general, this morphological interphase affects each of its phenomenological properties in a different manner, thus yielding interphases of different thicknesses for each property.

The observation that strong adhesive joints usually show cohesive failure delivers a substantial hint that phenomenological interphases can considerably exceed the nanometer scale. Cohesive failure means that the failure does not occur, as expected at first sight, at the immediate epoxy-metal boundary, but often tens to

hundreds of micrometers away from the interface within the polymeric network. There is of course no direct relationship between mechanical failure and linear elasticity as investigated by SBM. Nevertheless, the morphological properties of the interphase can be responsible for its mechanical interphase as well as for the cohesive failure behaviour. A first step towards the further elucidation of cohesive failure could be the spatial resolution of the linear mechanical properties of the related interphase.

In order to prove the existence of mechanical interphases at planar epoxy-metal boundaries, we probed at room temperature the hypersonic properties in the transitional zone between bulk epoxy and metals by means of $SBM^{\theta A}$ (SANCTUARY *et al*. 2003, KRÜGER *et al.* 2004a, 2005). The different metals did not only act as model substrates, but also as optical mirrors needed for the RIθA scattering geometry described in section 3.3 (KRÜGER *et al.* 1998). The influence of slight changes within the metal composition and morphology for the elastic interphase formation was studied for polymerizing amine-hardened glass-forming epoxies under identical conditions in contact with different planar aluminium surfaces (KRÜGER *et al.* 2005).

For the first sample type, the polished surface of a piece of aluminium typically used in workshops ('AlMgSi' made of 99.2 mass % Al, 0.4 mass % Mg and 0.4 mass % Si) was carefully rinsed with acetone and ethanol. For the second a physical vapour deposited aluminium surface, possessing its native oxide and adsorbate layers, was prepared. The two corresponding sound velocity profiles determined in the x_3-direction, perpendicular to the planar epoxy-aluminium interface, are given in figure 5.2. Apparently totally different acoustic and hence mechanical profiles develop in dependence of the aluminium surface properties. On the surface of the bulk aluminium alloy no detectable elastic interface appears; bulk epoxy properties are recorded directly from the interface up to a point located 0.6 mm away from the metal surface.

In contrast at the boundary of the physical vapour deposited aluminium an acoustic epoxy interphase extends over roughly 0.2 mm. Within this interphase, the longitudinal sound velocity shows a maximum value at $x_3 \approx 0.1\,\mathrm{mm}$, which lies about 3% higher than the bulk epoxy value. This corresponds to a longitudinal

modulus difference of as much as roughly 6%. The hypersonic attenuation profiles behave inconspicuously for both metal-epoxy joints (not shown in figure 5.2), which indicates that hypersonic relaxations are not at the origin of the differing elastic properties of both samples. To conclude this comparative study, two at first sight quite similar substrate surfaces possess strongly varying hypersonic velocity traces after polymerisation of the epoxy. $SBM^{\theta A}$ is hence able to characterize mechanical interphases via their linear elastic properties, but it is difficult to predict a priori in how far mechanical interphases develop or not in dependence of the substrate's nature, its physicochemical treatment and the adhesive composition.

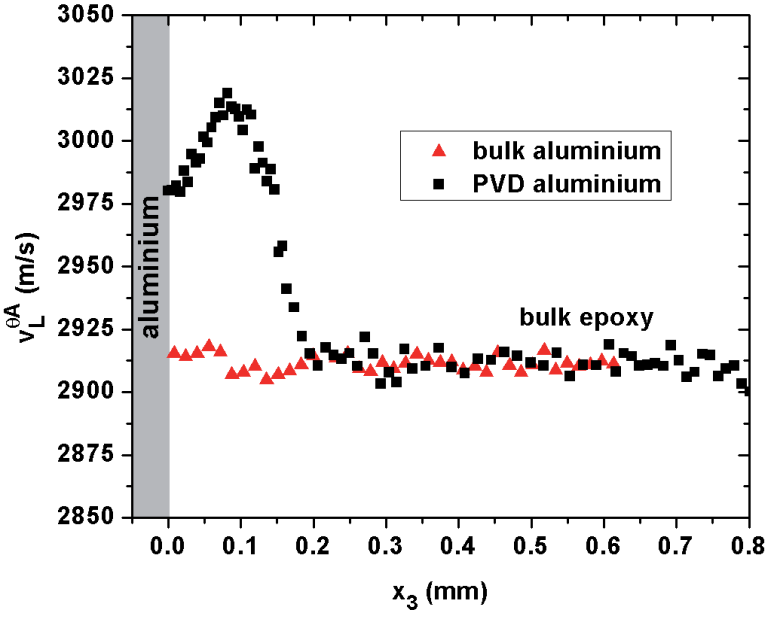

Fig. 5.2. Spatial sound velocity profiles within epoxies of the same composition glued to two different aluminium surfaces.

The prerequisites for the formation of an elastic epoxy interphase are either morphological differences inside the epoxy or non-linear elastic behaviour that influences second order elasticity via internal stress or strain fields (see section 4.5). None of both mechanisms seems to play a relevant role in the epoxy polymerized on

the bulk aluminium substrate. The formation of a maximum sound velocity 0.1 mm in front of the physical vapour deposited aluminium substrate indicates that for this sample at least two mechanisms need to be accounted for. Probably both aforementioned mechanisms superpose close to the substrate. The accompanying local minimum at the substrate's surface shows that both mechanisms affect the hypersonic velocity in opposite directions. As the considered epoxy shrinks about 5% during room temperature polymerization, we expect that especially close to the rigid metallic substrate mechanical stresses can build up in the epoxy. Shrinkage-induced stresses should start to develop when the epoxy possesses form-stability, i.e. after the occurrence of the sol-gel transition, and should become especially relevant at the glass transition. The obtained sound velocity profile probably reflects frozen-in non-equilibrium morphologies, which can at least partially be annealed by a post-polymerisation process (KRÜGER *et al.* 2005).

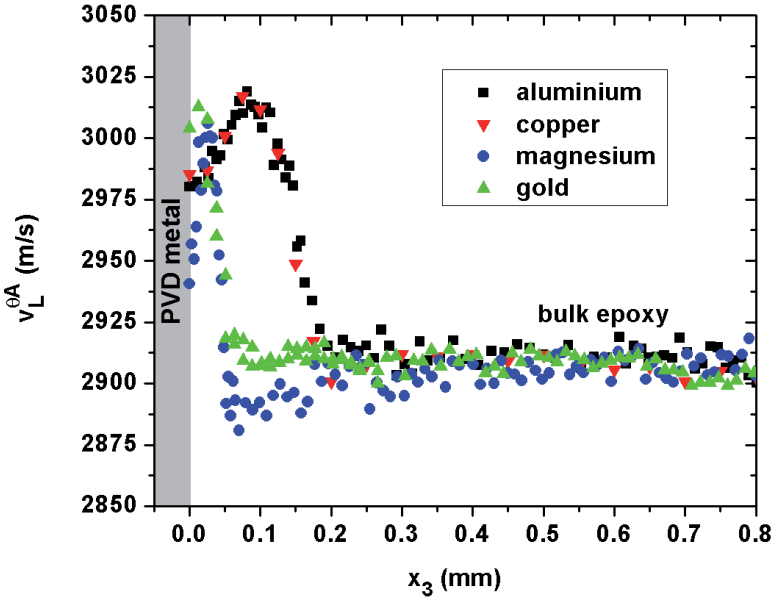

Fig. 5.3. Spatial sound velocity profiles within epoxies of the same composition glued to different physical vapour deposited metals at $x_3 = 0$ *mm*.

In order to test the occurrence of morphological changes within the polymeric network originating from metal-specific physicochemical interactions going beyond the creation of surface-induced stress or strain fields, mechanical interphases were investigated for the epoxy polymerised in contact to different physical vapour deposited metals. Figure 5.3 shows that mechanical interphases do not only appear on physical vapour deposited aluminium, but also arise in copper, magnesium and gold adhesive joints.

Considering the above-discussed huge difference in interphase formation for the two epoxy-aluminium samples, the similarity of the mechanical interphases' shape and extension (of some hundred microns) on the physical vapour deposited metal substrates is striking. The sound velocity maximum observed at least some tens of microns away from the metal substrates demonstrates that probably both above mentioned mechanisms, morphological differences and non-linear elastic behaviour resulting from stress fields, are again active. The absence of any oxidized layer on the gold substrate could potentially be taken as an argument for the sound velocity maximum being positioned close to the gold substrate and being dominated by mechanical stresses. However, this argument does not hold true for the epoxy-magnesium sample shown in figure 5.3, for which physicochemical processes should be much more relevant than on the epoxy-gold sample even though the extension of the interphases are comparable.

Meanwhile the existence of mechanical interphases in epoxy-metal joints has been endorsed by other teams using e.g. micro-scale indentation (MUNZ *et al.* 2005, ROCHE *et al.* 2006). The complexity of the interplay between interfacial interactions, matter transport processes, structure formation etc. does usually prevent a straightforward data interpretation. In this context, $SBM^{\theta A}$ has proven to be a versatile technique, able to spatially resolve interface-induced mechanical interphases. In order to deepen the scientific understanding on this field, we will extend our investigations and intend to couple them to more structure-sensitive experimental techniques.

5.3. Polymerisation of a two-component liquid and accompanying interphase formation in a mould with semi-permeable walls

In the previous sections two mechanisms of interphase formation basing on purely interfacial interactions were presented: first transcrystallization of a semi-crystalline polymer at a steel boundary and second adhesive bonding of an epoxy at different metal substrates. In both cases only the surface, but not the bulk of the metal substrates acts as a stimulus for interphase formation in the adjacent polymer; a modification of the metal's interior can be excluded. Especially for the examples of adhesive bonding, we have seen that the rigid metal substrates provoke interface-induced mechanical stresses in the epoxy networks, hiding to a certain extent possible interface-induced morphological changes.

In the study elucidated below, dealing with an epoxy polymerized within a silicone rubber cuvette, none of these restrictions holds true. Since the silicone rubber is only permeable for the hardener diethylene triamine (DETA), transport of DETA molecules from the polymerizing epoxy into the silicone rubber happens (MÜLLER *et al.* 2008). This results in a competition between selective matter transport processes and coexistent polymerization processes. These competing processes lead to a spatially varying epoxy network density, causing spatial changes of the elastic properties of the epoxy. As demonstrated below by $SBM^{\theta A}$ studies, the spatial evolution of the elastic properties of the polymerized epoxy gives to a certain extent insight into the preceding redistribution of the hardener and its integration in the epoxy network via covalent bond formation. But first a short introduction into the sample preparation and the polymerization process is necessary prior to the discussion of hypersonic data.

The same two-component, almost stoichiometric epoxy system as discussed in section 5.2 is polymerized at room temperature within a silicone rubber mould, or cuvette, with rectangular planar walls (MÜLLER *et al*. 2008). The cuvette's interior dimensions are $10\times10\times0.6\,mm^3$ and the wall thickness is 1 mm. After filling the liquid well-mixed epoxy into the silicone cuvette, the latter is covered with a lid made of the same material. The epoxy hardener DETA is known to easily penetrate

into the selected silicone rubber because of a strong chemical affinity between both components. There is no evidence that the resin diglycidyl ether of bisphenol A (DGEBA) or the oligomers formed during polymerization penetrate into the silicone rubber. The resulting DETA concentration gradient influences of course the epoxy reactions, and hence the formed network structures and their acoustic properties. After room temperature polymerization, a post-polymerization step (POSSART 2005) at 393 K was added in order to achieve the highest possible chemical conversion of the heterogeneous epoxy network. As no adhesive interaction between the epoxy and the silicone rubber occurs, interface-induced stresses are not expected to modify mechanical interphases within the epoxy. The $SBM^{\theta A}$ investigations were performed in the 90A scattering geometry along a scanning trace between the large faces of the epoxy sample located at $x_3 = -0.3$ mm and $x_3 = 0.3$ mm.

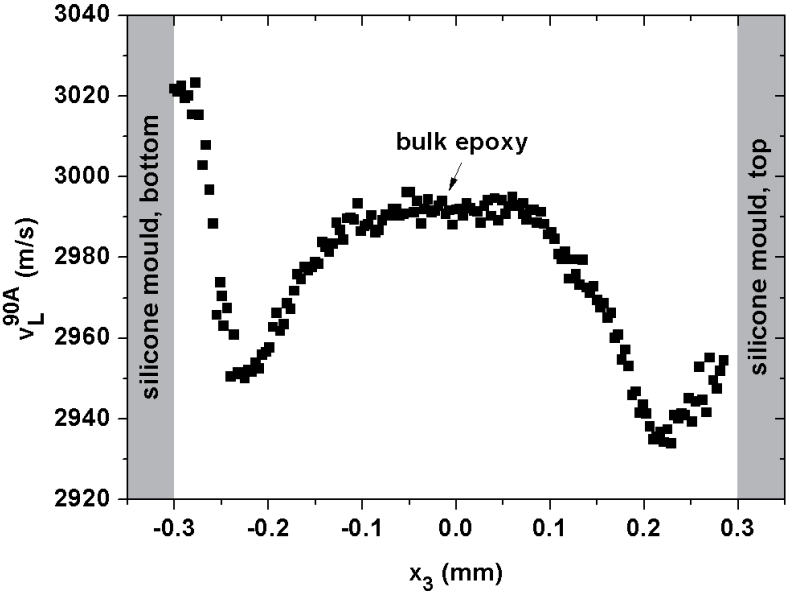

Fig. 5.4. Sound velocity profile recorded on a scanning trace through a 0.6 mm thick epoxy plate, prepared in a silicone rubber mould.

The corresponding acoustic profile is depicted in figure 5.4. Obviously, the hypersonic velocity profile is W-shaped and is asymmetric with respect to the geometrical symmetry plane of the epoxy sample positioned at $x_3 = 0$ mm. The central part of the hypersonic velocity profile reflects the usual hypersonic velocity $v_L^{90A} \approx 2990$ m/s of post-polymerized, almost stoichiometric bulk epoxy as measured in the 90A scattering geometry (KRÜGER *et al.* 2007). Consistent with the infrared spectroscopic findings (POSSART *et al.* 2006, WEHLACK *et al.* 2007, MEISER 2010, MÜLLER *et al.* 2010), sound velocities, which deviate from 2990 m/s, are attributed to differently cross-linked epoxy compared to the bulk. The W-shape of the sound velocity profile results from a complex interplay between selective molecular transport and covalent network formation. The following explanations concentrate on the bottom part of the epoxy plate (see left part of figure 5.4), as the composition of epoxy reactants within the upper part is falsified by DETA evaporation through the bearing face of the badly sealed silicone lid.

The selective DETA transport into the silicone rubber is initially driven by a limited miscibility of the epoxy components (ELLIS 1993) and highly different chemical affinities of the epoxy reactants for the silicone rubber. This provokes the hardener to penetrate into the silicone rubber, leading to an increasing opacity of the initially transparent silicone rubber. As, at the same time the adjacent epoxy zone is depleted in hardener, the epoxy reaction goes on slower in this region (MÜLLER *et al*. 2010). With progressing polymerization, the hardener concentration strongly decreases in the epoxy regions next to the interface. Accounting in addition for the increasing compatibility of DETA with larger epoxy fragments compared to DGEBA oligomers, the involved chemical affinities actually provoke that the hardener partially diffuses back from the silicone rubber into the reacting epoxy. The meanwhile created epoxy fragments hinder the DETA from flowing back over large distances into the epoxy.

The profile depicted in figure 5.4 reflects the finally realized spatial variation of the resin-hardener composition in the post-polymerized epoxy. In accordance with (KRÜGER *et al.* 2005, 2007, MÜLLER *et al.* 2010) sound velocities larger than the bulk epoxy value $v_L^{90A} \approx 2990$ m/s are attributed to epoxy networks

with slightly increased hardener concentrations compared to the DETA content of almost stoichiometric bulk epoxy, whereas smaller sound velocities reflect slightly increased resin concentrations. Of course, the dimensions and the geometry of the epoxy sample and of the silicone mould determine the competition between the aforementioned processes, the resulting final epoxy structures and their elastic properties.

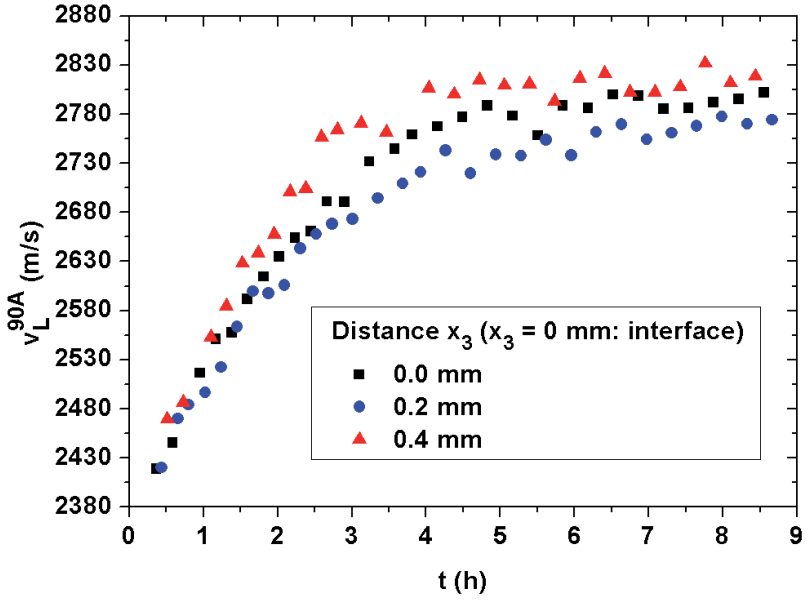

Fig. 5.5. Spatio-temporal sound velocity evolution, determined at three positions inside an epoxy specimen polymerizing at room temperature within a silicone rubber mould. The epoxy-silicone interface is located at $x_3 = 0.0$ *mm* .

Up to now, all conclusions about transient matter transport and polymerization processes have been drawn from the spatial distribution of the hypersonic velocity of the final epoxy sample. Time-resolved SBM measurements would be extremely helpful to study non-equilibrium processes in condensed matter that couple to linear elastic properties. For instance, the spatio-temporal acoustic evolution of liquid-

polymer interface systems could allow a unique perspective on the interplay between different matter transport and structure formation processes occurring in the vicinity of planar phase boundaries. In the following we describe the first time-resolved SBM investigation which we carried out and which retains the acoustic evolution of an epoxy polymerizing close to a silicone rubber boundary (MÜLLER *et al.* 2008).

As the involved silicone mould had different dimensions than the one discussed above, a quantitative comparison between both studies is impossible. Taking into account that the polymerization of the used epoxy typically takes some hours and that the recording of a BRILLOUIN spectrum lasted some minutes for this study, the temporal evolution of the sound velocity was resolved at only three positions within the polymerizing epoxy in close vicinity to the cuvette walls; more precisely at the epoxy-silicone interface $x_3 = 0.0$ mm, at $x_3 = 0.2$ mm and finally at $x_3 = 0.4$ mm (MÜLLER *et al.* 2008).

These first time-resolved $SBM^{\theta A}$ investigations are depicted in figure 5.5. During the first hour, the sound velocity growth determined at the three positions is almost identical. In the specified spatial range of 0.4 mm there seem to be no significant differences in the DETA concentration. At $x_3 = 0.4$ mm, the sound velocity development over the measured 9 h resembles that of the overall bulk composition (KRÜGER *et al.* 2007). Hence, the interface-induced processes mainly act in a zone less than 0.4 mm thick, next to the interface. As after more than two hours, the sound velocities increase quicker at the phase boundary than 0.2 mm within the epoxy, a higher hardener concentration is present just at the interface after these times. This can only be understood if after 2 h of polymerization the hardener already flows back from the silicone rubber into the epoxy. The increased hardener concentration leads to a quicker polymerization and slightly higher final values of the sound velocity. Shorter recording times for reliable BRILLOUIN spectra are necessary to improve the time-resolving capability of SBM. As demonstrated below, the SBM^{180-2D} setup described in section 3.2 allows overcoming this problem.

5.4. Solvent influence on epoxy networks: diethylene triamine and water

In the previous section it was shown that under the given experimental circumstances the hardener DETA can penetrate from outside into the polymerizing epoxy. This aspect will be explored in greater detail in chapter 6. In the following, we examine to which extent solvents like DETA and water can penetrate into polymerized epoxies and how this solvent-enrichment of the epoxy modifies its elastic properties. In particular the influence of water on the elastic properties of epoxies is of technological importance. SBM^{180-2D} is actually well suited to illustrate the spatial and temporal penetration of solvents into polymers by the related changes of the elastic properties. Note that this innovative SBM application permits a unique and highly promising perspective of elastic property modifications inaccessible by other experimental techniques (PHILIPP *et al.* 2009, 2011, SANCTUARY *et al.* 2010).

According to thermodynamics, the solvent uptake is always driven by the chemical affinity between the polymer and the solvent; however the interactions between both are not specified within this phenomenological approach (JONES 2002, CRANK 1975). Diverse solvent-polymeric network interactions, like ionic interactions, Van der Waals interactions, hydrogen bonds, etc. must generally be considered. For the amine-hardened epoxy and the solvents water and DETA, hydrogen bonds are regarded as being the most relevant interactions (SOLES & YEE 2000, MUSTO *et al.* 2002). There are lots of open questions in this research field concerning the state of adsorbed solvents: do free solvent molecules, i.e. solvent molecules which do not interact with the polymeric network exist within the voids of the polymer structure, how do the solvent molecules interact with the already existing hydrogen bonds of the epoxy network, and which different binding states of the solvent molecules do exist? Another question deals with the influence that the solvent molecules dissolved in the polymeric network have on the mechanical properties of the epoxy.

Experimentally, the solvent uptake is often characterized by integral methods, which determine e.g. the mass increase versus time of a polymer piece of

known dimensions immersed in a solvent. A drawback of such methods is that no spatial resolution of the solvent uptake process can be obtained. Figure 5.6 depicts the corresponding curves for post-polymerized, amine-hardened, almost stoichiometric epoxy pieces with the dimensions $10\times5\times1\,\mathrm{mm}^3$ immersed at room temperature in water or DETA, respectively. In case of water, the maximal mass increase corresponds to about 3 to 4% which is consistent with literature data (PETRIE 2006). The time needed for reaching saturation depends of course strongly on the solvent itself, the geometry, the chemical composition of the epoxy piece and external parameters like temperature. According to figure 5.6, the DETA uptake of the epoxy occurs much quicker than the water uptake under the given conditions. Within two months the mass of the epoxy piece swollen with DETA even increases by about 16% and the network is still not saturated by the solvent. DETA swells the initially glassy epoxy piece so much that it becomes gelatinous and breaks into pieces. Under these conditions the increase of the sample's weight is difficult to determine. This explains why the error bars are chosen much bigger for the epoxy immersion experiment in DETA than in water.

The conclusion of these immersion experiments is the following: Whereas the much more important DETA uptake of the epoxy compared to the water uptake represents a valuable outcome, it gives no information on more specific and essential properties like the spatial and temporal distribution of the penetrated solvent and the relevance of the local solvent enrichment for phenomenological properties, like the elastic moduli. Only a few experimental techniques like infrared spectroscopy and neutron scattering allow for the detection of the spatial advance of the diffusive solvent front within the polymer (LINDSAY *et al.* 1994, WAPNER & GRUNDMEIER 2004). But even these techniques can only give crude hints about the impact of the solvent sorption on phenomenological properties.

In contrast, SBM allows for gaining a unique spatio-temporal perspective on the solvent uptake at planar polymeric network-solvent interfaces. Indeed, on the one hand this technique does not interfere with the non-equilibrium matter transport and structure formation processes occurring within the sample and hence does not modify these processes. On the other hand, the hypersonic or mechanical properties

depend on the molecular interaction forces and the sample's mass density, which both can vary upon solvent uptake of the polymeric network. Thus SBM definitely possesses the potential to help clarifying the mechanical property evolution and the underlying processes occurring during solvent uptake of polymeric networks. However, note that elastic properties, like other phenomenological quantities, are always averages and give at best indirect information about microscopic interactions.

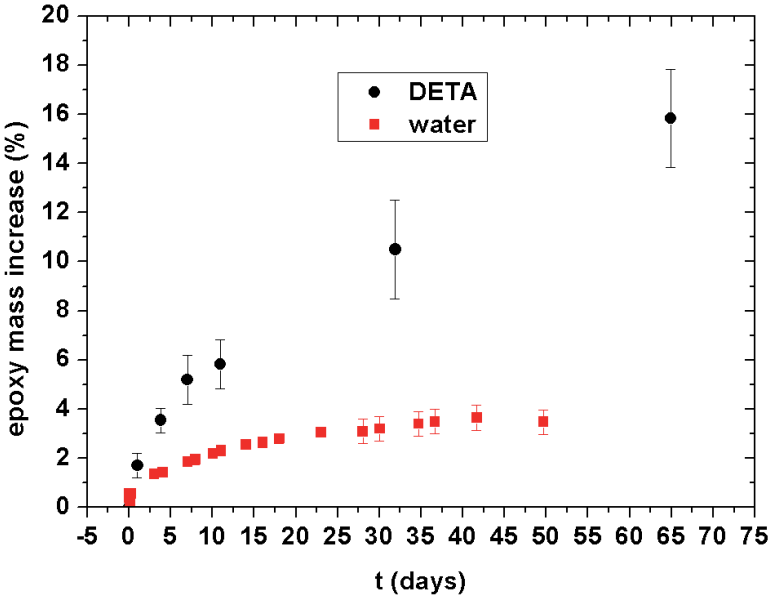

Fig. 5.6. Solvent uptake at room temperature of post-polymerized epoxy plates having the dimensions $10\times5\times1\ mm^3$ while being totally immersed in the solvent.

An almost planar epoxy-DETA interface with an area of $10\times10\ mm^2$ was created by filling an under-stoichiometric DGEBA/DETA (100/5) mixture at room temperature in a rectangular glass cuvette, which was topped by pure DETA (PHILIPP *et al.* 2011). After polymerization of the epoxy in the bottom compartment of the cuvette (see also section 6.1), the spatial and temporal sound velocity

evolution was recorded by means of SBM^{180-2D} (see section 3.2). In order to probe the advance of DETA into the epoxy, the hypersonic properties across the epoxy-DETA interface were repeatedly scanned along the same vertical scanning trace along x_1 as depicted in figure 3.2 (PHILIPP *et al.* 2011).

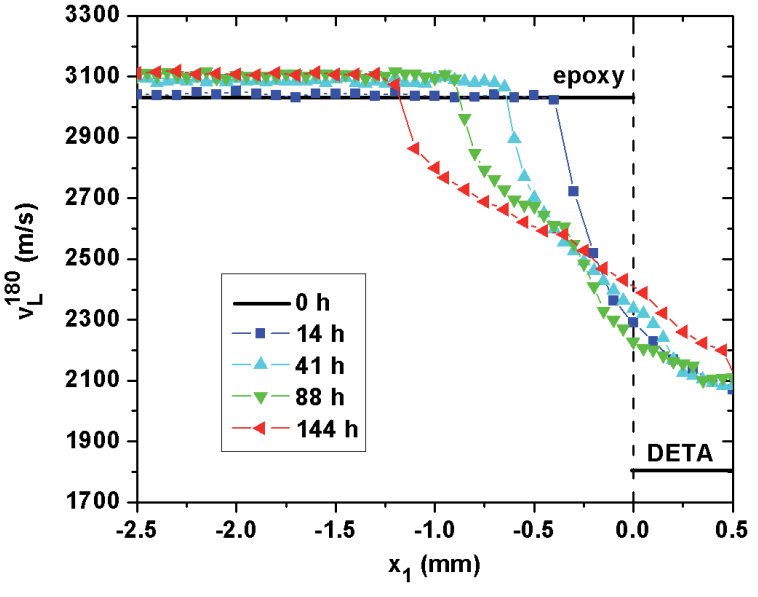

Fig. 5.7. DETA uptake of a room temperature polymerized, under-stochiometric epoxy at a planar phase boundary located at $x_1 = 0$ *mm*.

Figures 5.7 and 5.8 display the hypersonic perspective of the DETA uptake by the under-stoichiometric epoxy. The typical values for the polymerized epoxy and DETA (PHILIPP *et al*. 2011) are indicated as black lines in figure 5.7 and should illustrate the initial situation of the experiment. The slight sound velocity increase of 80 m/s observed within the bulk epoxy results from the slowly on-going polymerization in the glassy epoxy network. Concerning the interaction of DETA with epoxy at the glassy epoxy interface, it turns out that the more DETA penetrates into the epoxy, the more the sound velocity decreases. Hence, we conclude that not only

at low probe frequencies, but also at GHz frequencies the epoxy gets softer during DETA swelling. From a qualitative point of view this tendency may appear evident, but the water uptake experiment discussed below will exemplarily show that it is not. In figure 5.7 the sound velocity values of about 2300 m/s observed for the epoxy close to the initial interface correspond to typical values for gelatinous epoxy (SANCTUARY *et al.* 2010, PHILIPP *et al.* 2011). After 144 h the epoxy interphase provoked by DETA penetration into the epoxy has a thickness of about 1.2 mm within the bottom compartment. But this interphase is not confined to the original epoxy compartment, but also extents into the upper DETA-rich compartment. In other words, the epoxy entered the DETA-rich compartment while the solvent was swelling the polymeric network.

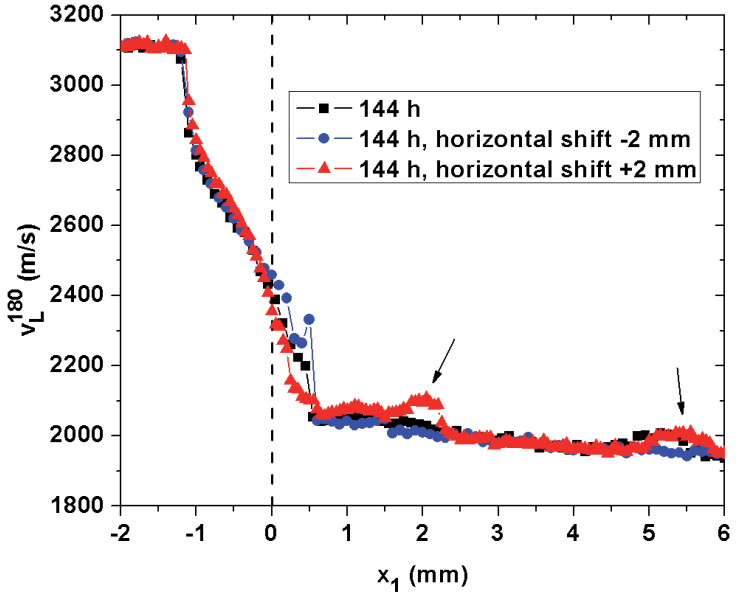

Fig. 5.8. Three vertical sound velocity profiles recorded after shifting the cuvette horizontally along z_2 (see fig. 3.2).

The spatial scans of figure 5.8 extend over a much larger scanning trace of about 8 mm. The sound velocity profile given in black evolves continuously with a complex shape, which indicates the action of competing transport and structure formation processes (see also section 6.1). Note that a rather sharp edge in the sound velocity profile exists at the interface between glassy epoxy and swollen, gelatinous epoxy located at $x_2 = -1.2$ mm. This steep descend indicates that the softening of the originally glassy epoxy is not just due to a smooth DETA gradient within the epoxy but that probably strong morphological changes in the epoxy network have happened (PHILIPP *et al*. 2011).

Performing a kind of BRILLOUIN imaging by horizontally shifting the whole cuvette prior to recording the vertical scans reveals that the majority of lateral heterogeneities occur within the upper compartment of the cuvette. Indeed, for the red curve we observe small sound velocity bumps located about 2 mm, respectively 5.5 mm above the initial interface (indicated by arrows). Hence the sound velocities have not only increased within the upper compartment due to epoxy oligomers being rinsed out of the epoxy network positioned at $x_1 < 0$ mm, but also swollen epoxy network fragments seem to be present at the mentioned locations. According to a recent publication (PHILIPP *et al.* 2011), the rupture of the epoxy network in the layered system is probably caused by lateral shear stresses that build up at the interface between glassy epoxy and gelatinous epoxy, which is swollen by DETA molecules. The inherent stochastic nature of these processes is responsible for the non-predictable character of the epoxy network rupture.

The investigation of the interphase of another epoxy-DETA sample substantiates the assumption that the sound velocity bumps indicated in figure 5.8 really correspond to swollen epoxy fragments. As a matter of fact during the 16 h considered in figure 5.9, the sound velocity bumps keep their shapes and seem to move upwards by about 1 mm. A possible explanation is as follows (PHILIPP *et al.* 2011): epoxy pieces located close to the glassy epoxy interface swell due to DETA penetration and increase in volume. The swelling-induced volume expansion lifts all the material placed on top of the swelling epoxy fragments. Furthermore, the upwards transport of these clearly shaped sound velocity bumps proves that

SBM^{180-2D} is especially suited for visualizing the transport of solid materials within liquids! In particular, if both substances have similar refractive indices, but sufficiently differing acoustic properties, SBM is a unique and handy experimental facility.

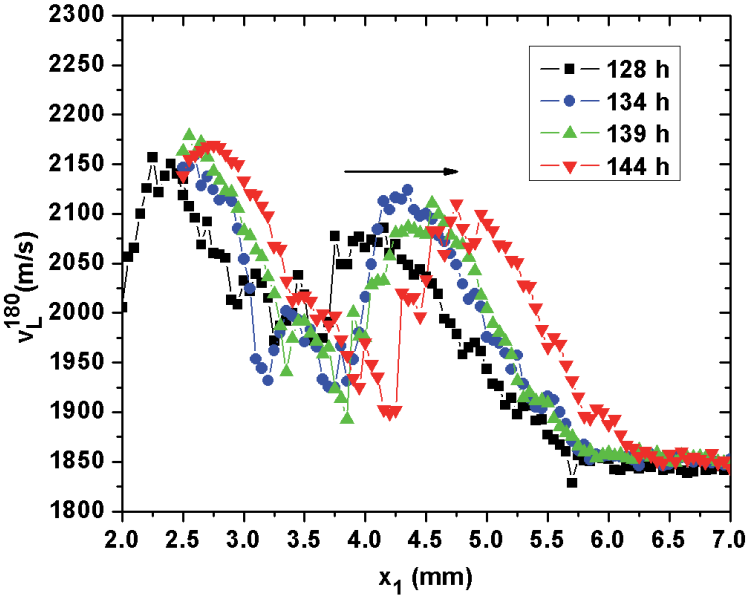

Fig. 5.9. Upwards transport of swollen epoxy fragments within a DETA-rich environment at room temperature.

Only recently the SBM^{180-2D} investigations have been extended towards the water uptake by the same epoxy class in order to elucidate whether water acts in a similar way as DETA does with epoxies. For that purpose an almost planar epoxy-air interface of the dimension $10\times10\ mm^2$ was first created by polymerizing an amine-hardened, almost stoichiometric glass-forming epoxy at room temperature in a glass cuvette with rectangular walls. After adding distilled water on top of the planar epoxy surface, the sound velocity evolution was recorded along a vertical scanning trace in the bottom epoxy-rich compartment by means of SBM^{180-2D}. Figure 5.10

shows representative profiles of the two-dimensional water uptake by the epoxy. The origin of the vertical x_1-axis, corresponding to $x_1 = 0$ mm, is fixed at the initial epoxy-water interface, negative x_1-values correspond to the epoxy compartment.

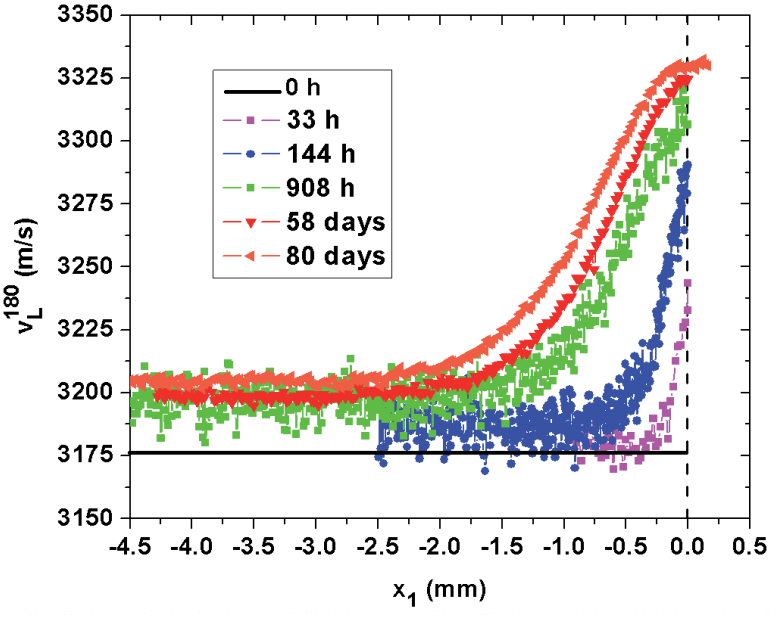

Fig. 5.10. Sound velocity profile of the room temperature water uptake of an epoxy at a planar phase boundary located at $x_1 = 0$ *mm*.

The higher smoothness of the profiles recorded after 58 and 80 days of the experiment results from an improvement of the data acquisition system. Note that the sound velocity of water corresponds to 1580 m/s and is of course much lower than that of glassy epoxy. As indicated by the horizontal line for the 0 h profile, the sound velocity of the undisturbed bulk epoxy is equal to ≈ 3180 m/s. After 33 h of the experiment, the sound velocities of the epoxy are only modified within a 0.2 mm thick zone at the phase boundary. The water penetration into the epoxy network

unexpectedly leads to a sound velocity increase by about 2%. As this value for sure does not correspond to usual simple mixing rules for both materials, strong intermolecular interactions between the epoxy network and water probably need to be accounted for. During the subsequent weeks, the shape of the spatial profiles remains similar. After 80 days of the experiment, the water has penetrated about 2 mm into the epoxy according to the sound velocity evolution. The definitely occurring increase of sound velocity observed with a growing water concentration seems to be in contradiction to the overwhelming majority of reports in literature (e.g. ITO *et al.* 2005, FERGUSON & QU 2006) that claim that the elastic moduli decrease under such conditions.

Whether this apparent contradiction is due to the high-frequency nature of BRILLOUIN spectroscopy or may be caused by internal stresses built up within the network during water penetration is currently an open question. After 80 days, the water infiltration into the epoxy network has led to network swelling so that the polymer reaches until about 0.2 mm within the upper compartment. The sound velocities level in this interphase zone at a value which is about 4% higher than that of the bulk epoxy. This is about a quarter of the total sound velocity increase during polymerization of this composition and corresponds to an increase of the longitudinal modulus of about 8%. It remains unclear whether the levelling of the sound velocity after roughly 80 days is related to a state of maximum water concentration within the epoxy network or whether other processes account for the sound velocity levelling. Another open question concerns the continuous sound velocity increase with time deep inside the epoxy: is it caused by a slowly ongoing polymerization within the glassy epoxy, or by water infiltration? Additional thorough SBM investigations performed over longer times on post-polymerized epoxies could help to answer these questions.

Finally simple immersion experiments let us conclude that under the same geometrical conditions and external parameters the DETA uptake of the amine-hardened epoxy is much more important than that of water. This result is in line with the stronger and quicker sound velocity changes observed for DETA penetration into the epoxy compared to the water uptake. Really remarkable is the fact that these

sound velocity changes have opposite signs. The underlying reasons for the so important DETA uptake by the epoxy may result from the interactions of DETA with epoxy and hydroxide groups due to the high reactivity of the amine groups of DETA. In order to gain further insight into physicochemical processes as those described above, a combination of SBM with structure-resolving methods, based e.g. on infrared spectroscopy or RAMAN spectroscopy could be of special benefit.